

ON THE CONSISTENCY OF NEUTRON-STAR RADIUS MEASUREMENTS FROM THERMONUCLEAR BURSTS

DUNCAN K. GALLOWAY^{1,2,3} & NATHANAEL LAMPE¹

Monash Centre for Astrophysics (MoCA), Monash University, VIC 3800, Australia

Accepted by ApJ

ABSTRACT

The radius of neutron stars can in principle be measured via the normalisation of a blackbody fitted to the X-ray spectrum during thermonuclear (type-I) X-ray bursts, although few previous studies have addressed the reliability of such measurements. Here we examine the apparent radius in a homogeneous sample of long, mixed H/He bursts from the low-mass X-ray binaries GS 1826–24 and KS 1731–26. The measured blackbody normalisation (proportional to the emitting area) in these bursts is constant over a period of up to 60 s in the burst tail, even though the flux (blackbody temperature) decreased by a factor of 60–75% (30–40%). The typical rms variation in the mean normalisation from burst to burst was 3–5%, although a variation of 17% was found between bursts observed from GS 1826–24 in two epochs. A comparison of the time-resolved spectroscopic measurements during bursts from the two epochs shows that the normalisation evolves consistently through the burst rise and peak, but subsequently increases further in the earlier epoch bursts. The elevated normalisation values may arise from a change in the anisotropy of the burst emission, or alternatively variations in the spectral correction factor, f_c , of order 10%. Since burst samples observed from systems other than GS 1826–24 are more heterogeneous, we expect that systematic uncertainties of at least 10% are likely to apply generally to measurements of neutron-star radii, unless the effects described here can be corrected for.

Subject headings: stars: neutron — X-rays: bursts — X-rays: individual(GS 1826–24) — X-rays: individual(KS 1731–26) — techniques: spectroscopic

1. INTRODUCTION

Interest has been raised in recent years in the prospects of inferring the neutron-star mass and radius from thermonuclear bursts. Such a possibility can provide stringent constraints on the neutron-star equation of state, which remains uncertain (e.g. Lattimer & Prakash 2007). From combining measurements of the blackbody normalisation (from time-resolved X-ray spectral fits to the burst spectra), Eddington luminosity, and the distance, confidence limits on the mass and radius of several neutron stars in low-mass X-ray binaries (LMXBs) has been estimated (Özel et al. 2009; Güver et al. 2010a,b; Özel et al. 2011; see also Steiner et al. 2010). Each of these quantities is challenging to measure alone, but particularly substantial systematic errors are known to affect the blackbody normalisation. The normalisation can rise or fall steadily throughout the burst tail, depending roughly on the duration of the burst (Bhattacharyya et al. 2010). Furthermore, in some sources different bursts provide significantly different normalisation values. Güver et al. (2011) quantified some of these effects at the 3–7% level, although in an earlier analysis of the burst source EXO 1745–248 found apparent radii measured from two bursts varying by 11% (Özel et al. 2009). Additionally, analysis of bursts from another globular cluster source, 4U 1724–307, found blackbody normalisations which varied by a factor of ≈ 2 (i.e. a 40% variation in the inferred radius) between short- and long-duration bursts (Suleimanov et al.

2011a).

Independent of the issues for measurement, are uncertainties about precisely how the neutron star’s atmosphere affects the emerging radiation. Although the burst spectra are typically found observationally to be consistent with a blackbody (e.g. Swank et al. 1977; Kuulkers et al. 2002), scattering effects have long been understood to distort the spectrum sufficiently to bias the measured temperature (e.g. London et al. 1984, 1986). This distortion is usually parameterised via a spectral distortion factor $f_c = T_{\text{bb}}/T_{\text{eff}}$ where T_{bb} is the measured blackbody (or colour) temperature, and T_{eff} is the effective temperature of the atmosphere. Most recent work adopt a narrow range of $f_c = 1.3$ – 1.4 at burst luminosities well below the Eddington limit (e.g. Madej et al. 2004), and often neglect the variations in f_c that may arise during the burst (e.g. Suleimanov et al. 2011b). A more rigorous approach involves fitting the observed variation in the blackbody normalisation (in response to the changing f_c) as a function of flux (e.g. Suleimanov et al. 2011a), although the predicted model curves cannot yet reproduce the range of observed behaviour.

Samples of bursts accumulated from individual sources can be extremely heterogeneous in their properties. From low-duty cycle observations featuring gaps due to Earth occultations and other conditions, it is usually impossible to be confident about the burst recurrence time, in which case the detailed ignition conditions, fuel composition, and even the completeness of thermonuclear burning are also uncertain. Under such conditions, it is difficult to disentangle the various systematic influences which might influence the normalisation measurements (e.g. Güver et al. 2011). Here we investigate the intrinsic reproducibility of burst normalisation measurements

Duncan.Galloway@monash.edu

¹ School of Physics, Monash University

² also School of Mathematical Sciences, Monash University

³ ARC Future Fellow

using a uniform, homogeneous sample of bursts, from the low-mass X-ray binaries GS 1826–24 and KS 1731–26. We use *Rossi X-ray Timing Explorer (RXTE)* Proportional Counter Array (PCA) data to test for intrinsic systematic effects which might influence burst normalisation measurements beyond any additional effects which might arise from variations in the ignition conditions and fuel composition. In a related paper, Zamfir et al. 2011 (submitted to ApJ; hereafter Z11) used the same data to infer the mass and radius of GS 1826–24.

2. OBSERVATIONS AND ANALYSIS

Few bursting sources exhibit trains of bursts with consistent lightcurves or recurrence times. The best known example is GS 1826–24, so far unique for its consistently regular burst behaviour, and high degree of uniformity between successive burst lightcurves (e.g. Galloway et al. 2004). Comparison of the burst behaviour and lightcurves suggest that the system accretes mixed helium and hydrogen at roughly solar mass fraction (Heger et al. 2007). We used observations of GS 1826–24 taken with the Proportional Counter Array (PCA; Jahoda et al. 1996) onboard the *Rossi X-ray Timing Explorer (RXTE)*, from the catalogue of bursts detected over the mission lifetime (Galloway et al. 2008; hereafter G08). The flux-recurrence time relationship for this sample has been extensively studied by Thompson et al. (2008). Optical photometry of the mass donor suggests an orbital period of 2.25 hr (Meshcheryakov et al. 2010). However, several alias peaks are present in the periodogram, and it is possible one of these (particularly at 2.05 hr) represents the true orbital period.

We performed a search of the G08 sample for additional examples of regular, consistent bursts. Recurrence time provides the most obvious way to detect regular bursts, although for instruments in low-Earth orbit like *RXTE*, recurrence time measurement is confounded by regular interruptions due to occultations of the star by the Earth. An alternative approach is to test for consistency of the burst light curve, via commonly-used parameters measuring the duration. The ratio τ of the fluence E_b to the peak flux, as used by G08, provides a simple way of comparing light curves. A scatter plot of τ against E_b for a source with consistent bursts, will show strong clustering, and KS 1731–26 provides the next best example after GS 1826–24. Extensive observations of KS 1731–26 by the *BeppoSAX/WFC* suggest that, at times, this system exhibits regular bursts more frequently than GS 1826–24 (see e.g. Fig. 3 from Cornelisse et al. 2003). Despite this, little attention has been directed at the burst behaviour of this system. One reason is that, unlike GS 1826–24, KS 1731–26 exhibits both radius-expansion bursts, and burst oscillations (Muno et al. 2000); previous analyses have focussed largely on these phenomena. A series of *RXTE* observations of KS 1731–26 were made in 2000 August and September, detecting a total of 14 bursts with highly consistent lightcurves. *WFC* observations also made during this time show that the burst behaviour was quite regular, with recurrence times of between 2–3 hr. An additional example, with a lightcurve very similar to those observed in 2000, was detected on 1999 Aug 26. Soon after the 2000 observations, the source faded to quiescence,

and has not been active since (Wijnands et al. 2001).

No other sources exhibit clustering as tight in the rest of the G08 sample; the next best examples are 4U 1323–62 and 4U 0836–429. 4U 1323–62 is quite well-known for its regular burst behaviour (e.g. G08), and in the *RXTE* sample, many of the bursts were long with $\tau = 28 \pm 2$ s and similar fluences, of $E_b = (100 \pm 10) \times 10^{-9}$ erg cm⁻². However, several of the bursts were closely followed by weaker events only a few minutes after the first. This behaviour has been observed in a number of systems (e.g. Keek et al. 2010), and is thought to arise from delayed ignition of material left over from the initial burst. Such events are likely not suitable for a detailed test of the consistency of blackbody normalisations between bursts. During a period of activity in 2003–4, 4U 0836–429 exhibited long ($\tau = 22 \pm 4$ s) bursts at roughly similar fluences, distributed approximately as a Gaussian with $E_b = (270 \pm 70) \times 10^{-9}$ erg cm⁻². Despite good coverage of the outburst, the bursts were apparently not strictly periodic in nature, and there may also be contributions to the source flux from a nearby HMXB pulsar which is within the PCA field of view. Thus, we also exclude this source from our study.

Where not explicitly stated, the data analysis procedures are as in G08. Time-resolved spectra in the range 2–60 keV covering the burst duration were extracted on intervals as short as 0.25 s during the burst rise and peak, with the bin size increasing gradually into the burst tail to maintain roughly the same signal-to-noise level. A spectrum taken from a 16-s interval prior to the burst was adopted as the background. We re-fit the spectra over the energy range 2.5–20 keV using the revised PCA response matrices, v11.7⁴ and adopted the recommended systematic error of 0.5%. The fitting was undertaken using XSPEC version 12. In order to accommodate spectral bins with low count rates, we adopted Churazov weighting. No correction for instrumental deadtime was applied to the spectra.

We modelled the effects of interstellar absorption, using a multiplicative model component (**wabs** in XSPEC), with the column density n_H frozen at 4×10^{21} cm⁻² (for GS 1826–24, e.g. in 't Zand et al. 1999) and 1.3×10^{22} cm⁻² (for KS 1731–26, e.g. Cackett et al. 2006). In the original analysis carried out by G08, the neutral absorption was determined separately for each burst, from the mean value obtained for spectral fits carried out with the n_H value free to vary. This has a negligible effect on the fluxes, but can introduce spurious burst-to-burst variations in the blackbody normalisation. We also computed averaged lightcurves of blackbody spectral parameters for subsets of bursts from GS 1826–24, following the procedure adopted by Galloway et al. (2004).

3. RESULTS

We first explored a variety of different approaches to measuring the blackbody normalisation in the tail of the bursts. We used an event from GS 1826–24 on 2000 July 1 17:16:37 (#12 in G08). Four of five PCUs (0–3) were functioning for this burst. We took the approach of iteratively determining the maximum extent in the tail (beginning from a few seconds after the burst start)

⁴ see `\protect`<http://www.universe.nasa.gov/xrays/programs/rxte/pca/doc/rmf/pcarmf-11.7>

Table 1
Different approaches for determining the mean blackbody normalisation

Treatment	Mean K_{bb} [(km/ $d_{10\text{kpc}}$) ²]	Time range (s)	kT range (keV)	Flux range [10^{-9} erg cm ⁻² s ⁻¹]	χ^2_{ν} (DOF)
averaged, variable bins	103.3 ± 0.7	3.0–65.25	2.32–1.55	28.69–6.09	1.45 (95)
joint fit, variable binsize	107.0 ± 1.1	11.50–32.25	2.16–1.79	24.26–11.80	1.13 (942)
averaged, 0.25-s bins	103.5 ± 0.7	3.25–50.75	2.32–1.46	28.69–7.05	1.28 (186)
joint fit, 0.25-s bins	105.5 ± 0.9	4.75–32.00	2.32–1.72	28.69–11.18	1.08 (2460)

over which a constant fit to the blackbody normalisations was an acceptable fit to below 3σ confidence. We refer throughout to the best-fit constant value as $\langle K_{\text{bb}} \rangle$, to distinguish from the individual K_{bb} values for each time-resolved spectrum.

We found a best-fit value of $\langle K_{\text{bb}} \rangle = 103.3 \pm 0.7$ (km/ $d_{10\text{kpc}}$)² over the interval 3.0–65.25 s (relative to the start over the burst; Fig. 1). The reduced $\chi^2/n_{\text{DOF}} \equiv \chi^2_{\nu}$ was 1.45, for 95 degrees of freedom. Remarkably, this consistency was maintained despite the fitted blackbody temperature kT_{bb} falling from 2.32 to 1.55 keV.

In order to double-check our result, we carried out a similar procedure to determine the maximum extent over which the blackbody normalisation was consistent with a constant value, but instead of simply averaging the fitted normalisations for each time bin, we performed a joint fit in XSPEC of the time-resolved spectra to an absorbed blackbody model, as used for the individual spectra. We froze the neutral column density at the same value as used for the individual spectral fits, 4×10^{21} cm⁻². We linked the blackbody normalisation for each of the individual spectra but allowed the blackbody temperatures to vary. With this treatment, the fitted $K_{\text{bb, joint}}$ was found over a shorter time interval, between 11.5–32.25 s following the burst start, and at a 3% higher value of 107.0 ± 1.1 (Table 1). Likely, the higher value is attained by omitting some of the spectra in the range 40–60 s, when there is a noticeable downward trend in the normalisation (Fig. 1). We note that the mean of the normalisation values over the reduced extent of the burst permitted by the joint fits, returns a consistent best-fit value, of 106.6 ± 1.1 .

The fact that the two treatments returned a different extent of the burst tail over which the normalisation was constant may be attributed to the degree of goodness of fit of the individual spectra. The distribution of χ^2 for the individual fits in the time range 3.0–62.5 s following the burst start is shown in Fig. 2. Compared to the expected distribution given the number of degrees of freedom (22), the observed distribution is skewed significantly to higher values of χ^2 . This result suggests that residual systematic errors (either instrumental, or possibly from deviations from a blackbody) prevented a joint fit to the same confidence level extending over the same extent of the burst tail, compared to the simple average.

We also explored the effect of the time binning approach on the results, by repeating the two analyses on data which used uniform 0.25 s bins throughout the burst. The bin sizes for the G08 data were 0.25-s from the start of the burst through to 14.5 s after the start, 0.5 s to 24.5 s, 1 s to 43.25 s, and 2 s through to 65.25 s. We found that the $\langle K_{\text{bb}} \rangle$ value obtained with uniform

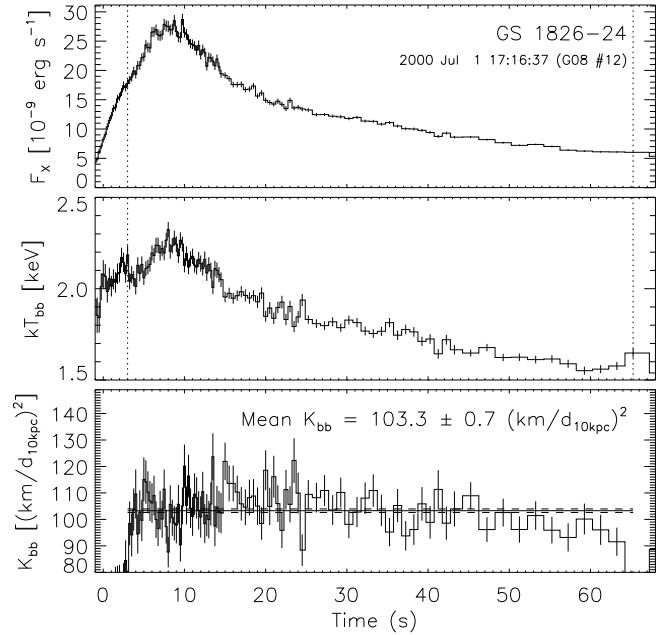


Figure 1. Example burst observed by *RXTE* from GS 1826–24 on 2000 July 1 17:16:37 UT (#12 in G08), illustrating the constancy of the blackbody normalisation over a significant extent of the burst tail. Shown is the burst flux (*top panel*), blackbody (colour) temperature kT_{bb} (*middle panel*), and blackbody normalisation (in units of (km/ $d_{10\text{kpc}}$)²; *bottom panel*). The extent over which the constant-normalisation fit is calculated is illustrated by the vertical dotted lines (*top and middle panels*), and the horizontal lines (*lower panel*), with the 1σ error range indicated (*dashed lines*). The reduced- $\chi^2 = \chi^2_{\nu}$ for the constant fit is 1.45, for $\nu = 95$ degrees of freedom.

0.25-s bins was identical to that with bins of variable size, although the extent of the constant fit was slightly less (extending to 50.75 s instead of 65.25 s; Table 1). Similarly, the joint fit to the uniform 0.25-s binned spectra gave a comparable result to the joint fit for variable bins, and over roughly the same extent of the burst. The χ^2 distribution for the 0.25 s-binned data over the range 3.25–50.75 s after the burst start was similarly discrepant from the expected distribution assuming a statistically good fit, but at a lower confidence level (K-S statistic of 0.12, equivalent to 2.5σ).

The *RXTE* PCUs are subject to a short ($\approx 10 \mu\text{s}$) interval of inactivity following the detection of each X-ray photon. This “deadtime” reduces the detected count rate below what is incident on the detector (by approximately 3% for an incident rate of $400 \text{ count s}^{-1} \text{ PCU}^{-1}$). For GS 1826–24, the bursts peak at $\approx 2500 \text{ count s}^{-1} \text{ PCU}^{-1}$, giving a peak dead-time rate of $\approx 6\%$ (reducing in the burst tail to $\approx 4\%$

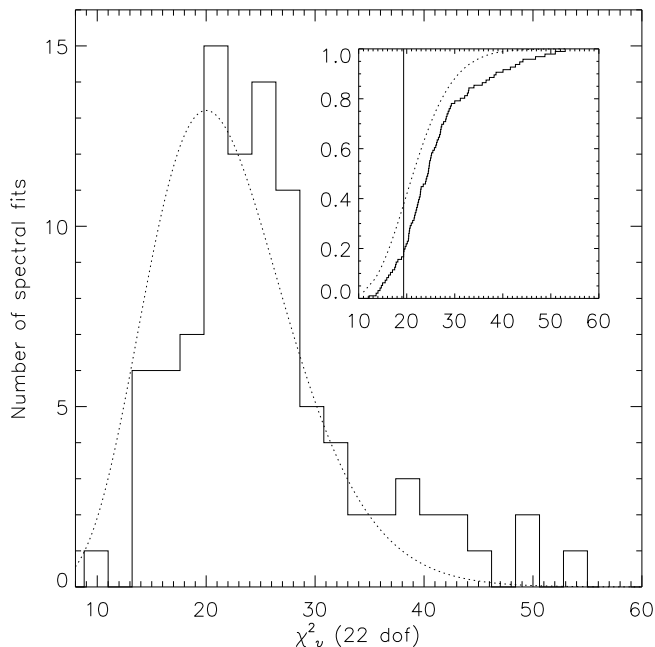


Figure 2. Distribution of fit statistic χ^2 for blackbody fits to time-resolved spectra from burst #12 from GS 1826–24, on 2000 July 1 17:16:37, over the time for which the blackbody normalisation was determined to be constant (3.0–65.25 s relative to the burst start). The expected distribution for statistically acceptable fits with 22 degrees of freedom is overplotted (*dotted line*). The fit χ^2 show an excess of high values, as also indicated by the cumulative probability distributions (*inset*); a K-S test returns a value of 0.21, indicating disagreement at the 3.4σ level.

after ≈ 60 s). Since the bursts reach approximately the same peak flux, the deadtime correction is also approximately the same, and can be neglected for comparison purposes (we similarly neglect any issues related to the absolute PCA calibration). However, since the deadtime correction varies with time, it might also be expected to result in a slightly different evolution of the normalisation throughout the burst. To test this possibility, we examined the duration of the constant interval for the burst analysed in this section (#12 from G08), with and without the deadtime correction. Although we measured an increase in the average normalisation with the deadtime correction, as expected, we found no change in the extent over which the normalisation was found to be constant. Thus, we neglect deadtime corrections for the remainder of the analysis in this paper.

3.1. The full burst sample from GS 1826–24

We analysed 67 bursts observed from GS 1826–24 by *RXTE* between 1997 and 2007. This sample includes the set of 58 complete bursts in G08, excluding seven events for which the full lightcurve was not observed, or for which no appropriate data modes were available for the analysis, and one event which occurred during a slew and for which the burst flux could not be determined correctly⁵. We also analysed an additional 9 bursts from observations in 2006 August, which were not part of the G08 sample.

We compared the results of the joint fits $K_{\text{bb},\text{joint}}$ with

the average of the individual fits $\langle K_{\text{bb}} \rangle$ for the bursts from this sample to determine how the results from our sensitivity tests translated to a larger sample. Although in some cases the joint fit durations were shorter than the constant fit duration for the individual normalisations the median duration was 94% of the average interval. Furthermore, we found no systematic difference between the normalisations determined by the two methods, and the agreement was at better than 2% for 76% of the measurements (maximum deviation was 8.5%). This compares favourably to the typical 1σ statistical uncertainty on the measurements, of 1%. Thus, we conclude that the parameter averages $\langle k_{\text{bb}} \rangle$ provide an unbiased measure of the blackbody normalisation in the tail of these bursts, and adopt that method for further analysis.

The $\langle K_{\text{bb}} \rangle$ for the bursts from GS 1826–24 determined from the individual spectral fit parameters (using the spectra with variable binsizes; see §3) is shown in Fig. 3. The typical span of the constant fit was from < 3 s after the burst start (52% of the bursts) to approximately 60 s. For one burst the normalisation was found to be constant from 2–77 s after the start of the burst; the median duration was 48 s. Over the interval during which the blackbody normalisation was constant, the blackbody temperature typically decreased from 2.3 to 1.6 keV, while the flux decreased from $\approx 3 \times 10^{-8}$ erg cm $^{-2}$ s $^{-1}$ to $\approx 5 \times 10^{-9}$ erg cm $^{-2}$ s $^{-1}$.

The $\langle K_{\text{bb}} \rangle$ values were not significantly correlated with either the duration over which the average was calculated, nor the maximum time out to which the average was calculated. Interestingly, the earliest time to which the constant fits could be extended (≈ 1 –3 s after the burst start) was within the ≈ 5 s burst rise. For several of the bursts, the time at which the normalisation reaches the mean value corresponds approximately to a change in slope of the burst rise, seen in several of the bursts (e.g. Fig. 1). This feature is similar to the “bump” seen in model lightcurves (e.g. Heger et al. 2007). Although in the simulations this feature must arise due to some variation in the rate of increase of thermonuclear energy production (as the 1-D models cannot account for lateral propagation), the coincidence of the observed change in slope with the normalisation achieving its mean value suggests that this point marks where the effects of spreading cease. Further analysis of the detailed shape of the burst rises may help to clarify this situation.

We found significant variations in the mean normalisation $\langle K_{\text{bb}} \rangle$, both between and within different observational epochs. For the bursts within each epoch (1997–8 and 2000–7), the normalisation varied by 5 and 4%, respectively. This variation was highly significant; the χ^2 values for constant fits were 218 (for 6 degrees of freedom) and 1007 (for 59 degrees of freedom), respectively. In terms of the inferred radius, this implies systematic uncertainties of order 2–2.5%. Additionally, a much larger variation was measured between the two epochs. The first seven bursts, observed between 1997 November and 1998 June, had $\langle K_{\text{bb}} \rangle$ values substantially larger than the remaining bursts (observed from 2000 June onwards). The mean and standard deviation for the normalisations of the 1997–8 bursts was 118 ± 6 (km/ $d_{10\text{kpc}}$) 2 while for subsequent bursts was 101 ± 4 (km/ $d_{10\text{kpc}}$) 2 . A two-

⁵ The excluded bursts are #8, 15, 21, 29, 39, 42, and 44 from Table 5 of G08

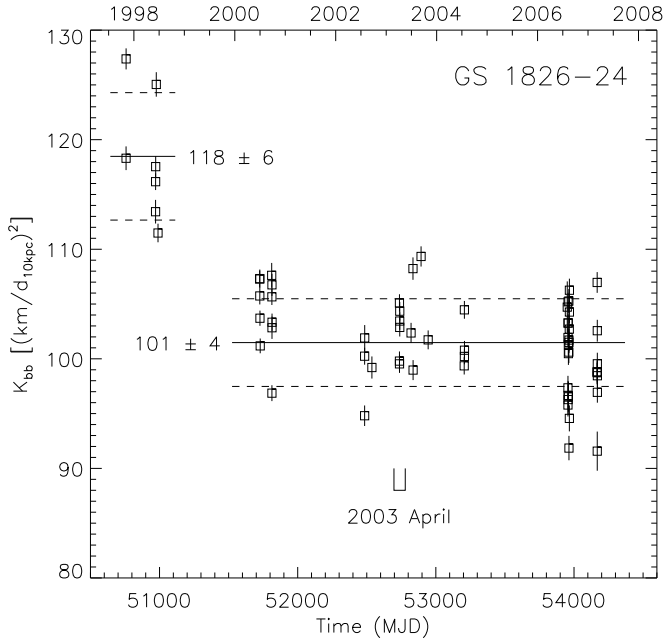


Figure 3. Mean blackbody normalisation values for 67 thermonuclear bursts observed by *RXTE* from GS 1826–24. The mean and standard deviation for the two observation epochs (1997–8 and 2000–7) are indicated. Note the marked discrepancy between the mean values for the two distributions; the K-S statistic indicate that they are discrepant at a significance of 1.3×10^{-6} , equivalent to 4.7σ .

sided Kolmogorov-Smirnov test confirms that these distributions are discrepant at the 1.3×10^{-6} significance level (equivalent to 4.7σ). This variation was also noted by Galloway et al. (2004), who reported instead a correlation between the persistent flux and the blackbody normalisation for a subset of the bursts analysed here.

The observed variation is unlikely to arise from any instrumental effect, as the PCA is precisely calibrated to maintain stable flux measurements for calibration sources over the entire mission lifetime. As we discuss below, the discrepancy is also unlikely to result from variations in the neutral column density n_H as a function of epoch. Closer examination of the spectral variation in the two groups of bursts provides a possible explanation. In contrast with the example burst discussed in the previous section, and other bursts observed in 2000–7, the constant fit interval for the bursts observed in 1997–8 began later than in the 2000–7 bursts; typically 10 s after the burst start for the 1997–8 bursts, compared to 3 s after the burst start for the other bursts. To put this another way, there was additional variation in the blackbody normalisation during the burst rise for the 1997–8 bursts that prevented extension of the constant interval to the same point as in the later bursts. This is illustrated in Fig. 4, which compares the blackbody normalisation averaged over the 1997–8 bursts with that of the 2000–7 bursts. Remarkably, however, the behaviour of the normalisation in the two groups of bursts is virtually identical during the burst rise; the discrepancy sets in from 10 s after the burst start, with the normalisation of the 1997–8 bursts gradually increasing over another ≈ 10 s to a higher level.

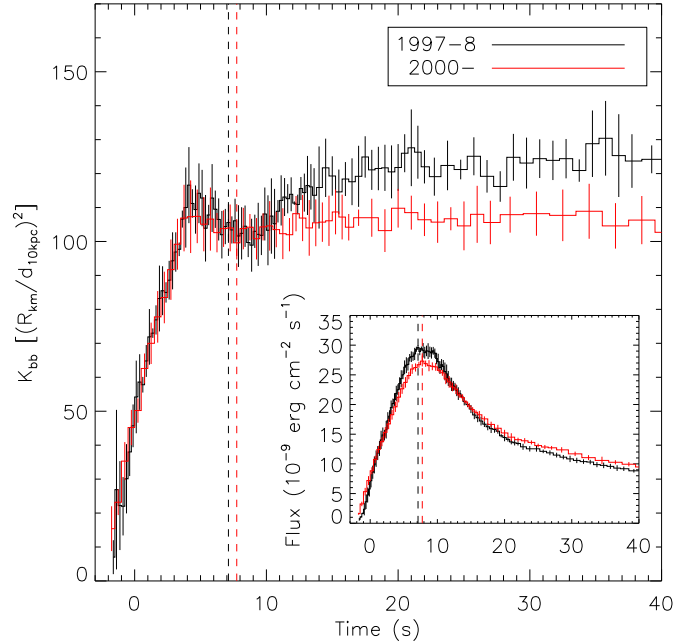


Figure 4. Comparison of averaged blackbody normalisation profiles for bursts from GS 1826–24 measured in 1997–8 (#1–5 of G08) and 2000–7 (#9, 10, 11, 12, 13, 16, 17, 19, 20). The vertical dashed lines indicate the time of maximum flux for each set of bursts. Note the agreement in the normalisation throughout the burst rise and maximum, and the increasing discrepancy from 10 s after the burst start. The inset shows the corresponding variation of the averaged burst flux.

3.2. KS 1731–26

RXTE observations of KS 1731–26 in 2000 August–September detected 14 bursts, 8 in August and 6 in September (these are bursts #14–21 and 22–27 in G08, respectively). Although the *RXTE*/PCA observations were interrupted regularly due to the satellite orbit and other scheduled observations, the times of the detected bursts were consistent with a regular recurrence time. The shortest burst separation measured by *RXTE* during each month of data was ≈ 2.5 hr; the longer separations were consistent with integer multiples of this value, indicating regular bursts where intervening events were missed within data gaps. We measured the average recurrence times based on linear fits to the burst arrival times measured by *RXTE*, as 2.577 ± 0.011 hr and 2.636 ± 0.003 hr for August and September, respectively. One further burst, observed on 1999 Aug 26 (#13 in G08), exhibited a lightcurve consistent with the 14 observed in 2000, and we included it in this sample.

The regular bursts featured similar long (≈ 5 s) rises and decays (≈ 60 s) as those typically observed from GS 1826–24 (Fig. 5). The peak count rate was ≈ 2300 count s^{-1} PCU $^{-1}$, so that deadtime corrections are comparable to those of GS 1826–24 (see §3). However, the recurrence time for the bursts from KS 1731–26, at ≈ 2.6 hr, were significantly shorter than has been observed from GS 1826–24 in years of *RXTE* observations (e.g. Thompson et al. 2008). Based on the assumed distances for the two sources (6 kpc for GS 1826–24 and 7.2 kpc for KS 1731–26; see G08), the bursts from KS 1731–26 reached significantly higher luminosities of $(1.8\text{--}1.9) \times 10^{38}$ erg s^{-1} , and the burst durations were also

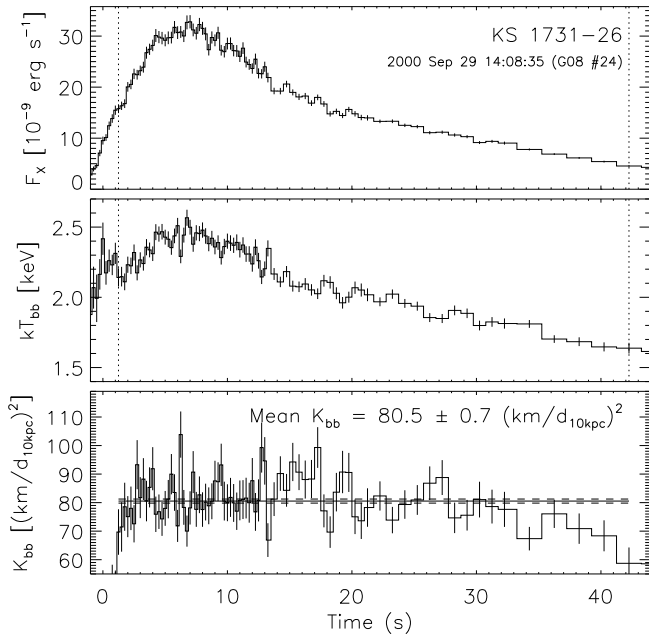


Figure 5. Example burst observed by *RXTE* from KS 1731–26 on 2000 September 29 14:08:35 UT (#24 in G08), illustrating the constancy of the blackbody normalisation over a significant extent of the burst rise and tail. Panel descriptions are as for Fig. 1. The reduced- $\chi^2 = \chi^2_\nu$ for the constant fit is 1.39, for $\nu = 79$ degrees of freedom.

significantly shorter ($\tau = 24$ s compared with ≈ 40 s for GS 1826–24). A shorter burst duration for KS 1731–26 suggests a smaller fraction of hydrogen in the burst fuel, although the shorter recurrence time also allows less hydrogen to be consumed by steady burning prior to the burst.

As with GS 1826–24, we measured the best-fit normalisation $\langle K_{\text{bb}} \rangle$ from the time-resolved blackbody spectral fits over the longest possible time interval without exceeding the 3σ confidence limit. With the shorter bursts from KS 1731–26, the constant K_{bb} fits extended typically over the range 2–30 s after the burst start. Over this time interval, the blackbody temperature dropped (typically) from 2.5 to 1.8 keV, with the flux dropping from 3×10^{-8} erg cm $^{-2}$ s $^{-1}$ to 7×10^{-9} erg cm $^{-2}$ s $^{-1}$.

The fitted $\langle K_{\text{bb}} \rangle$ values of the long bursts from KS 1731–26 exhibited significant variability; a fit with a constant model gave a $\chi^2 = 112.7$ for 14 degrees of freedom, indicating variability at the 8.5σ level. The mean value was 80 ± 2 (km/d $_{10\text{kpc}}$) 2 , with standard deviation between the various measurements of 2.6%. The mean blackbody normalisation of the burst on 1999 Aug 26, measured between 1.25–36 s after the burst start at 79.7 ± 0.8 (km/d $_{10\text{kpc}}$) 2 , was fully consistent with the bursts observed in 2000 despite being observed a year earlier.

In an independent analysis of the bursts observed from KS 1731–26 with *RXTE* (of which the bursts we analyse here are a subset), Güver et al. (2011) measured a mean blackbody normalisation of 88.4 ± 5.1 (km/d $_{10\text{kpc}}$) 2 , and found weakly significant variation in the normalisation as a function of the burst flux. Although this value is not significantly different from the normalisation we derive from the subset of bursts analysed here,

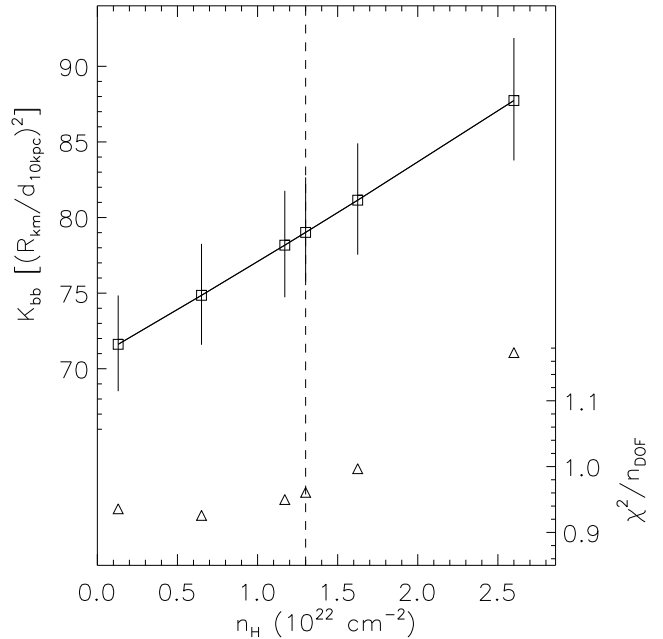


Figure 6. Sensitivity of the blackbody normalisation in spectral fits of *RXTE* data to the assumed column density n_H . The fits were calculated from a simulated spectrum with $kT = 2.1$ keV, including pre-burst persistent and instrumental background from burst #15 of KS 1731–26. The square symbols show the fitted value of the blackbody normalisation (left-hand y -axis) as a function of the assumed column density n_H . The lower half of the plot shows the corresponding χ^2 values; each fit is statistically acceptable. The choice of the n_H value can clearly introduce a systematic bias to the normalisation values, of the order a few per cent.

we suggest that the difference arises from a systematic effect due to the value adopted for the neutral column density. For the analysis presented here, we assumed $n_H = 1.3 \times 10^{22}$ cm $^{-2}$ (from multi-epoch *Chandra* and *XMM-Newton* spectra of the source during quiescence; Cackett et al. 2006) while Güver et al. (2011) adopted a value of 2.98×10^{22} cm $^{-2}$, the mean of best-fit values from fits to the burst spectra measured by *RXTE*. For a simulated blackbody spectrum with known kT and normalisation, adopting a realistic model for the pre-burst emission as background, the fitted value of the normalisation depends linearly on the assumed n_H (Fig. 6). That is, over (under) estimating the n_H value assumed for the fits will have the effect of over (under) estimating the K_{bb} . For the representative parameters chosen, the slope gives approximately 6.5 (km/d $_{10\text{kpc}}$) 2 for every additional 10^{22} cm $^{-2}$ in column that is adopted. The difference between the adopted values for the two analyses could account for an offset in the normalisations of up to 11 (km/d $_{10\text{kpc}}$) 2 , sufficient to explain the discrepancy.

4. DISCUSSION

We found significant variations in the blackbody normalisation $\langle K_{\text{bb}} \rangle$ averaged over tens of seconds of the burst tail in a homogeneous sample of regular, consistent bursts from GS 1826–24 and KS 1731–26, both within and between observation epochs. We found that the variation within epochs was 4–5% (2.6%) for GS 1826–24 (KS 1731–26), while the variation between epochs can be as large as 17% (for GS 1826–24). In terms of inferred radius, this corresponds to variations of 2–2.5% (1.3%) and

8%. The variation within each epoch is within the range reported by Güver et al. (2011) in their more comprehensive study of bursts from several sources, although the 8% variation between epochs observed for GS 1826–24 is somewhat larger. We stress that this uncertainty is solely related to the measurement of the blackbody normalisation in bursts, and (as suggested by Z11) may be exceeded by other sources of uncertainty, for example the degree of anisotropy of burst emission.

The 1997–8 bursts from GS 1826–24, which exhibited longer recurrence times and reached slightly higher fluxes, also exhibited larger mean normalisations ($\langle K_{\text{bb}} \rangle$). Comparison of the normalisation time-series averaged over subsamples of bursts from the two epochs show that the normalisations were essentially identical during the burst rise and through the burst peak, with deviations becoming apparent between 10–20 s after the burst start. The reproducibility of the K_{bb} evolution throughout the burst rise and peak suggests that the system geometry, atmospheric composition and temperature (and hence f_c) were essentially identical over that interval, and whatever physical condition gave rise to the elevated K_{bb} in the 1997–8 bursts set in after the burst peak. We consider three possible mechanisms to give rise to the variation.

First, it may be that the amount of neutral material close to the neutron star was reduced, so that the neutral column density n_H decreased during the 1997–8 bursts, leading to an overestimation of K_{bb} (see e.g. Fig. 6). Simulations adopting the pre-burst emission from GS 1826–24 (as was done for KS 1731–26; see §3.2) indicate that in order to overestimate the $\langle K_{\text{bb}} \rangle$ by the required amount would necessitate decreasing the total n_H value by $1.9 \times 10^{22} \text{ cm}^{-2}$. Since this value is almost five times the assumed line-of-sight value for GS 1826–24, we can rule out this mechanism.

Second, it is possible that the degree of anisotropy of the burst emission changed in response to a variation in the accretion geometry (e.g. Fujimoto 1988), perhaps triggered by the burst. Such a change might be expected to be reflected in the X-ray spectrum. The broadband ($\approx 1\text{--}100 \text{ keV}$) spectral distribution of the persistent emission in GS 1826–24 has been well studied by Thompson et al. (2008), in the context of determining the best possible estimate of the bolometric flux (and hence the accretion rate). Those authors found substantial changes in the spectrum with epoch, most notably during 2003 April, when evidence for an additional soft ($< 1 \text{ keV}$) component was found. However, the mean normalisation from the 6 bursts observed in 2003 April was $(102 \pm 4) (\text{km}/d_{10\text{kpc}})^2$ (see Fig. 3), fully consistent with the mean from the other bursts from 2000 onwards (but excluding the 2003 April bursts), of $(101 \pm 4) (\text{km}/d_{10\text{kpc}})^2$. Conversely, there is no evidence for a substantially different X-ray spectrum during the 1997–8 observations (see Thompson et al. 2008, Fig. 4). The lack of correspondence between the broadband spectral shape and the blackbody normalisation from the bursts seems to contraindicate an influence of the burst anisotropy on the normalisation, although cannot rule it out. On the other hand, the variations in the persistent X-ray spectrum might be transient, present only when the elevated K_{bb} values were measured, beginning 10 s

after the burst start. Such variations might be expected to lead to incorrect pre-burst emission subtraction later in the burst, although this is not observed consistently.

Third, we consider the possibility that the f_c value changes to produce the variation in the measured K_{bb} after the peak in the 1997–8 bursts from GS 1826–24. Modelling studies indicate that f_c depends on fixed parameters such as the neutron star surface gravity, but also the composition and effective temperature of the scattering atmosphere (e.g. Madej et al. 2004; Suleimanov et al. 2011b). There is evidence in other sources that radius-expansion bursts can remove the outer, H-rich layers of the photosphere, leading to a change in the atmospheric composition during the burst (Galloway et al. 2006); no such effects have been suggested from non-radius expansion bursts. Nevertheless, interpreting the maximum variation in $\langle K_{\text{bb}} \rangle$ in the 1997–8 bursts, compared to the mean for the 2000–7 bursts, as a variation in f_c implies a maximum variation of 12% (8% in the mean). This result suggests that the assumption that f_c is constant during bursts is not always true. While Suleimanov et al. (2011b) predict patterns of variation of f_c with burst flux, the epoch-to-epoch differences in the burst lightcurves in GS 1826–24 are relatively subtle, and do not appear sufficient to give rise to the inferred variation in f_c .

It is possible that the peak blackbody flux (or temperature) serves as the discriminant which results in elevated blackbody normalisations later in the burst. The 1997–8 bursts reached maximum fluxes about 8% higher on average than for the 2000–7 bursts. The discrepancy in the maximum temperature reached was proportionately smaller. The samples of bursts studied here were deliberately selected for the consistency of their lightcurves and regularity of their recurrence times. For other samples of bursts, which are typically much more heterogeneous, systematic errors in measurements of the blackbody radius of order $\gtrsim 8\%$ should be assumed, unless the variation in f_c can be modelled.

The mean blackbody normalisations measured during the later (2000–7) bursts from GS 1826–24, and the regular bursts from KS 1731–26, were consistent with a constant value over several tens of seconds. This constancy was observed independent of the specific method for determining the mean value, although the choice of method can introduce small biases. In particular, comparisons of joint fits to the spectra with averages of the fitted normalisations show that in general the former method arrives at shorter durations for the constant normalisation, likely because the spectra are not (en masse) statistically consistent with blackbodies. Trends in the blackbody normalisation late in the burst tail, coupled with these marginally deviant spectra, likely give rise to systematic errors of a few percent between the two methods. The choice of time binning strategy does not have as large an effect.

This constancy of the blackbody normalisation was maintained despite significant decreases in the blackbody temperature, of (typically) 30%, and decreases in the flux of 60–75% over the same time interval. Such a lack of variation in the blackbody normalisation implies constraints on the relative degree of spectral distortion over this temperature range, suggesting one of two situations. Either, any variation in the spectral

distortion factor f_c as a result of the varying effective temperature (as indicated by the decreasing blackbody temperature) is *exactly balanced* by some other variation, e.g. a change in the emitting radius as the burst flux decreases; or, that the color temperature correction f_c is also constant throughout the interval in which K_{bb} is constant. The former explanation is rather contrived, particularly considering that in the burst tail the burning front is expected to have already spread to the entire surface area of the neutron star, and no further increase (or decrease) in burning area is expected. Thus, these measurements suggest that for the range of effective temperatures spanned in the burst tails, the color-temperature correction f_c is roughly constant. This conclusion is difficult to reconcile with the predictions of atmosphere models (e.g. Suleimanov et al. 2011b), which indicate significant variations in f_c over most of the flux range spanned during the burst. The distance for GS 1826–24 is thought to be ≈ 6 kpc (Heger et al. 2007), at which an Eddington-limited burst would be expected to reach $F/F_{\text{Edd}} = 3.7 \times 10^{-8}$ (6.3×10^{-8}) $\text{erg cm}^{-2} \text{s}^{-1}$ for an H-rich (pure He) atmosphere (e.g. G08). This would imply that the range of flux over which the burst normalisation is found to be constant is 0.16–0.75 (0.10–0.46) F/F_{Edd} . The greatest variation in the normalisation predicted by Suleimanov et al. (2011a) is outside these ranges, although significant variations would yet be expected (particularly for the solar metallicity models; see also Z11).

The ≈ 3 –5% fractional variation in $\langle K_{\text{bb}} \rangle$ observed from GS 1826–24 and KS 1731–26 within each observational epoch was smaller than that seen in two radius-expansion bursts observed from EXO 1745–248, of 25% (Özel et al. 2009). This observation perhaps suggests an explanation of the variation. EXO 1745–248 exhibited during its 2000 outburst an initial period of strong variability, reminiscent of dipping behaviour observed in high-inclination systems (e.g. Galloway et al. 2008). No such variability has ever been observed from GS 1826–24 or KS 1731–26, suggesting that perhaps the inclination is lower in those systems than in EXO 1745–248. If system inclination is the main factor in determining the variation in apparent blackbody normalisation, a possible explanation is the reprocessing of some fraction of the burst flux off an accretion disk whose projected area varies with time. In 4U 1728–34, the timescale inferred for the variation was several tens of days (Galloway et al. 2003), much longer than the expected orbital period of this system (e.g. Galloway et al. 2010). However, in GS 1826–24 and KS 1731–26, the variation is on a much shorter timescale, comparable to the recurrence time of the bursts themselves (hours). For comparison, the discrepant bursts from EXO 1745–248 were separated by 8.5 d. We note that such an explanation fails to account for the factor of ≈ 2 difference in normalisation in the bursts from 4U 1724–307 (Suleimanov et al. 2011a), which does not show dips and thus is unlikely to be at high inclination. However, those bursts also exhibited markedly different timescales, indicative of a varying accumulated fuel reservoir at ignition; we suggest instead that different physical conditions (temperature, composition) gave rise to the difference in the measured blackbody normalisation.

The shorter timescale of variation in $\langle K_{\text{bb}} \rangle$ for GS 1826–24 and KS 1731–26 suggests that there may be an orbital component of the variation. The specific value of the blackbody normalisation depends upon the assumed neutral column density, as illustrated in Fig. 6. Thus, an orbital variation in the line-of-sight column density, perhaps arising from cool clouds of material above the point of contact of the accretion stream with the disk, will manifest as a variation in the blackbody normalisation on the same timescale. In order to test this hypothesis, we calculated a Lomb-normalised periodogram on the blackbody normalisation measurements as a function of time. Recall the orbital period in both sources is unknown, but for GS 1826–24 is thought to be around 2 hr; based on the typical orbital periods for other burst sources, we searched a frequency range of 0.5–24 hr. For GS 1826–24, we divided the measurements from the two epochs through by the appropriate mean, and found a peak Lomb power of 10.48; for KS 1731–26, we found a peak Lomb power of 5.29. Neither of these detections is significant. For KS 1731–26, the known sensitivity of the normalisation measurement to discrepancies between the assumed and true value of n_H indicates that a variation of $0.3 \times 10^{22} \text{ cm}^{-2}$ in n_H could account for the variation in the measured blackbody normalisation. For GS 1826–24, the measurements are slightly more sensitive to discrepancies in n_H , so that a variation in n_H of $0.45 \times 10^{22} \text{ cm}^{-2}$ could account for the variation in the blackbody normalisation within each epoch. If orbital or longer-timescale variations in n_H are driving the variation in the blackbody normalisation, it may be possible to verify through time-resolved high-spectral resolution measurements of absorption edges in the X-ray spectra.

We thank the anonymous referee, who made several substantial comments which improved the paper. DKG is a member of an International Team in Space Science on type-I X-ray bursts sponsored by the International Space Science Institute (ISSI) in Bern, Switzerland, and we thank ISSI for hospitality during part of this work. This research has made use of data obtained through the High Energy Astrophysics Science Archive Research Center Online Service, provided by the NASA/Goddard Space Flight Center. DKG is the recipient of an Australian Research Council Future Fellowship (project FT0991598).

Facilities: RXTE

REFERENCES

- Bhattacharyya, S., Miller, M. C., & Galloway, D. K. 2010, MNRAS, 401, 2
- Cackett, E. M., Wijnands, R., Linares, M., Miller, J. M., Homan, J., & Lewin, W. H. G. 2006, MNRAS, 372, 479
- Cornelisse, R., in 't Zand, J. J. M., Verbunt, F., Kuulkers, E., Heise, J., den Hartog, P. R., Cocchi, M., Natalucci, L., Bazzano, A., & Ubertini, P. 2003, A&A, 405, 1033
- Fujimoto, M. Y. 1988, ApJ, 324, 995
- Galloway, D. K., Cumming, A., Kuulkers, E., Bildsten, L., Chakrabarty, D., & Rothschild, R. E. 2004, ApJ, 601, 466
- Galloway, D. K., Muno, M. P., Hartman, J. M., Psaltis, D., & Chakrabarty, D. 2008, ApJS, 179, 360
- Galloway, D. K., Psaltis, D., Chakrabarty, D., & Muno, M. P. 2003, ApJ, 590, 999
- Galloway, D. K., Psaltis, D., Muno, M. P., & Chakrabarty, D. 2006, ApJ, 639, 1033

- Galloway, D. K., Yao, Y., Marshall, H., Misanovic, Z., & Weinberg, N. 2010, *ApJ*, 724, 417
- Güver, T., Özel, F., Cabrera-Lavers, A., & Wroblewski, P. 2010a, *ApJ*, 712, 964
- Güver, T., Psaltis, D., & Özel, F. 2011, accepted by *ApJ*; ArXiv e-prints 1103.5767v1
- Güver, T., Wroblewski, P., Camarota, L., & Özel, F. 2010b, *ApJ*, 719, 1807
- Heger, A., Cumming, A., Galloway, D. K., & Woosley, S. E. 2007, *ApJ*, 671, L141
- in 't Zand, J. J. M., Heise, J., Kuulkers, E., Bazzano, A., Cocchi, M., & Ubertini, P. 1999, *A&A*, 347, 891
- Jahoda, K., Swank, J. H., Giles, A. B., Stark, M. J., Strohmayer, T., Zhang, W., & Morgan, E. H. 1996, *Proc. SPIE*, 2808, 59
- Keek, L., Galloway, D. K., in't Zand, J. J. M., & Heger, A. 2010, *ApJ*, 718, 292
- Kuulkers, E., Homan, J., van der Klis, M., Lewin, W. H. G., & Méndez, M. 2002, *A&A*, 382, 947
- Lattimer, J. M. & Prakash, M. 2007, *Phys. Rep.*, 442, 109
- London, R. A., Taam, R. E., & Howard, W. M. 1984, *ApJ*, 287, L27
- . 1986, *ApJ*, 306, 170
- Majej, J., Joss, P. C., & Róžańska, A. 2004, *ApJ*, 602, 904
- Meshcheryakov, A. V., Revnivtsev, M. G., Pavlinsky, M. N., Khamitov, I., & Bikmaev, I. F. 2010, *Astronomy Letters*, 36, 738
- Muno, M. P., Fox, D. W., Morgan, E. H., & Bildsten, L. 2000, *ApJ*, 542, 1016
- Özel, F., Gould, A., & Güver, T. 2011, ArXiv e-prints 1104.5027v1
- Özel, F., Güver, T., & Psaltis, D. 2009, *ApJ*, 693, 1775
- Steiner, A. W., Lattimer, J. M., & Brown, E. F. 2010, *ApJ*, 722, 33
- Suleimanov, V., Poutanen, J., Revnivtsev, M., & Werner, K. 2011a, *ApJ*, 742, 122
- Suleimanov, V., Poutanen, J., & Werner, K. 2011b, *A&A*, 527, A139+
- Swank, J. H., Becker, R. H., Boldt, E. A., Holt, S. S., Pravdo, S. H., & Serlemitsos, P. J. 1977, *ApJ*, 212, L73
- Thompson, T. W. J., Galloway, D. K., Rothschild, R. E., & Homer, L. 2008, *ApJ*, 681, 506
- Wijnands, R., Miller, J. M., Markwardt, C., Lewin, W. H. G., & van der Klis, M. 2001, *ApJ*, 560, L159
- Zamfir, M., Cumming, A., & Galloway, D. K. 2011, ArXiv e-prints 1111.0347v1